Proceedings of ASME Turbo Expo 2011
GT2011
June 6-10, 2011, Vancouver, British Columbia, Canada

GT2011-45477

FILM COOLING ON HIGHLY LOADED BLADES WITH MAIN FLOW SEPARATION - PART 2: OVERALL FILM COOLING EFFECTIVENESS

Reinaldo A. Gomes[*]**, Reinhard Niehuis**
Institute of Jet Propulsion
University of the Federal Armed Forces Munich
85577 Neubiberg
Germany
Email: reinaldo.gomes@unibw.de

ABSTRACT

Film cooling experiments were run at the high speed cascade wind tunnel of the University of the Federal Armed Forces Munich. The investigations were carried out with a linear cascade of highly loaded turbine blades. The main targets of the tests were to assess the film cooling effectiveness and the heat transfer in zones with main flow separation. Therefore the blades were designed to force the flow to detach on the pressure side shortly downstream of the leading edge and it reattaches at about half of the axial chord. In this zone film cooling rows are placed among others for reduction of the size of the separation bubble.

The analyzed region on the blade is critical due to the high heat transfer present at the leading edge and at the reattachment line after main flow separation. Film cooling can contribute to a reduction of the size of the separation bubble reducing aerodynamic losses but increases in general heat transfer due to turbulent mixing. The reduction of the size of the separation bubble might also be twofold since it acts like a thermal insulator on the blade and reducing the size of the bubble might lead to stronger heating of the blade. Film cooling should therefore take into account both: firstly a proper protection of the surface and secondly reduce aerodynamic losses diminishing the extension of the main flow separation.

The overall effectiveness of film cooling for a real engine has to combine heat transfer with film cooling effect. In this paper the overall effectiveness of film cooling, combining results from measurements of the adiabatic film cooling effectiveness and the local heat transfer coefficient are shown. The tests comprise the analysis of the effect of different outlet Mach and Reynolds numbers at engine relevant values and film cooling ratio.

A new parameter is introduced which allows to evaluate the effect of film cooling accounting at the same time for the change of local heat transfer coefficient. To the authors' opinion this parameter allows a better, physically based assessment than the strategy using the so-called heat flux ratio. A parameter study is carried out in order to benchmark the effect of changes of the blade design.

NOMENCLATURE

c	Blade chord
c_p	Specific heat capacity at constant pressure
C_s	Sutherland constant=$1.458 \cdot 10^{-6}\,\mathrm{kg}/(\mathrm{m} \cdot \mathrm{s})$
K	Acceleration parameter
K_1	Geometrical and material constant = $k/\Delta y$
h	Blade height, heat transfer coefficient
k	Conductivity
Ma	Mach number
p	Pressure
Pr	Prandtl number
q	Dynamic head
$\dot{q}$	Heat flux
R	Ideal gas constant for air=$287\,\mathrm{J}/(\mathrm{kg} \cdot \mathrm{K})$
r	Recovery factor
Re	Reynolds number
S	Sutherland Constant=$110\,\mathrm{K}$
T	Temperature
t	Blade pitch
TDR	Temperature difference ratio
u	Velocity
x,y,z	Coordinate
α	Surface tangent angle
β	Angle
γ	Isentropic coefficient, angle
γ_r	Compound angle
η	Adiabatic film cooling effectiveness
θ	Non dimensional coolant temperature
ν	Kinematic viscosity
ξ	Temperature ratio $T_{w,in}/T_c$
φ	Non dimensional wall temperature = $1/\theta$

[*]Address all correspondence to this author.

Subscripts

∞	Outside the boundary layer
0	Non film cooled case
1	Cascade inlet plane
2	Cascade outlet plane
aw	Adiabatic wall
ax	Axial direction
c	Coolant, film cooled case
cyl	Cylindrical
fs	Fan shaped
in	Internal
r	Recovery
s	Isentropic
t	Total or stagnation condition
w	Wall

INTRODUCTION

Modern high pressure turbine blades are set under high thermal stress. The turbine inlet temperature has been increasing considerably since the early years of gas turbine manufacturing in order to increase the work output per unit mass and the thermal efficiency of the machine. Nowadays, the hot gas temperature in the first turbine stages can usually be well beyond acceptable metal temperatures and complex cooling techniques are used in order to keep the airfoils and endwalls at an affordable temperature, see e. g. Han et al. [1]. Film cooling is a well known technique and has been used for decades in turbomachines for protection of solid surfaces from hot gas. The costs of extracting a portion of compressed air and ejecting it from blades and endwalls bypassing the combustion chamber results in an overall cycle efficiency gain and many efforts were made in the past years in order to improve the cooling efficiency.

In recent years the development of blades with increased loading have led to lighter and cost-optimized products and efforts are being undertaken in order to continue the development of technologies for higher blade loading, see e. g. Haselbach and Schiffer [2] or Janke and Wolf [3]. In presence of very high blade loading flow separation is likely to occur and new techniques have to be developed in order to control the flow separation for both reasons the aerodynamic losses as well as surface cooling. Experiments have therefore been carried out at the University of the Federal Armed Forces Munich in order to assess the effect of film cooling on the total pressure losses as well as on the surface temperature of a highly loaded turbine blade with flow separation. The experiments are also used for validation and development of numerical tools.

The effect of film cooling can be investigated by measuring the reduction of the adiabatic wall temperature, which is usually described in terms of the adiabatic film cooling effectiveness η which for incompressible flow is defined by

$$\eta = \frac{T_\infty - T_{aw}}{T_\infty - T_c}. \tag{1}$$

Results for the measured adiabatic film cooling effectiveness on the pressure side of a highly loaded turbine blade with flow separation are shown in Gomes and Niehuis [4, 5]. In a real engine both the heating of the wall by heat transfer from the hot main flow and the cooling by the coolant flow influence the film cooled non-adiabatic wall temperature. In fact both flows, main and coolant flow, interact with each other and very often film cooling can enhance the heat transfer to the wall by strong mixing and therefore heat the wall compared to the case without film cooling. Hence the combination of both effects, film cooling and heat transfer, is needed in order to evaluate the impact of film cooling on local wall temperature. This can be done in several ways: One possibility is to measure the heat flux into the blade in a first run without and in a second run with film cooling by keeping the ratio of coolant to main flow temperature in the same order as on the real engine. Examples of this technique can be found in Camci and Arts [6] or Abhari and Epstein [7]. As soon as the wall temperature decreases, the heat flux into the blade decreases also while the temperature difference $T_\infty - T_w$ increases. Both lead to a lower heat transfer coefficient h defined in case of incompressible flow by

$$h = \frac{\dot{q}}{T_w - T_\infty}. \tag{2}$$

With another methodology, see Eckert [8], one can measure the adiabatic film cooling effectiveness in a first run. In a second run the local heat transfer coefficient h_c is measured with the film cooling temperature equal to the main flow temperature $T_c = T_\infty$, the so-called isoenergetic condition. In assuming linearity of the energy equation in dependence of the temperature the heat flux can then be obtained with

$$\dot{q} = h_c \cdot (T_w - T_{aw}) \tag{3}$$

while T_{aw} is obtained from eq. (1). One can of course also use eq. (3) in order to compute T_w for a given heat flux. Similar to the second approach is the method used by Choe et al. [9], which is called the superposition approach. Given constant wall and main flow temperatures one can measure the heat transfer coefficient at a random combination of heat flux and coolant temperature and obtain e. g. the heat transfer coefficient for isoenergetic condition h_c since the heat transfer coefficient has a linear relationship with respect to

$$\theta = \frac{T_c - T_\infty}{T_w - T_\infty}. \tag{4}$$

This allows also to compute the film cooling effectiveness for zero heat flux, but as the authors point out this film cooling effectiveness may defer from the adiabatic film cooling effectiveness measured on an adiabatic wall with changing wall temperature. Though the wall temperature was not kept constant in the experiments of Metzger et al. [10] the authors also show a linear agreement between h and θ.

The two last mentioned methods are well established and valuable ways of measuring the effect of film cooling on both parameters adiabatic film cooling effectiveness and heat transfer coefficient as well as to compute the heat flux for a given combination of coolant, main flow and wall temperature. But it seems to be difficult to compare the film cooled with the case without

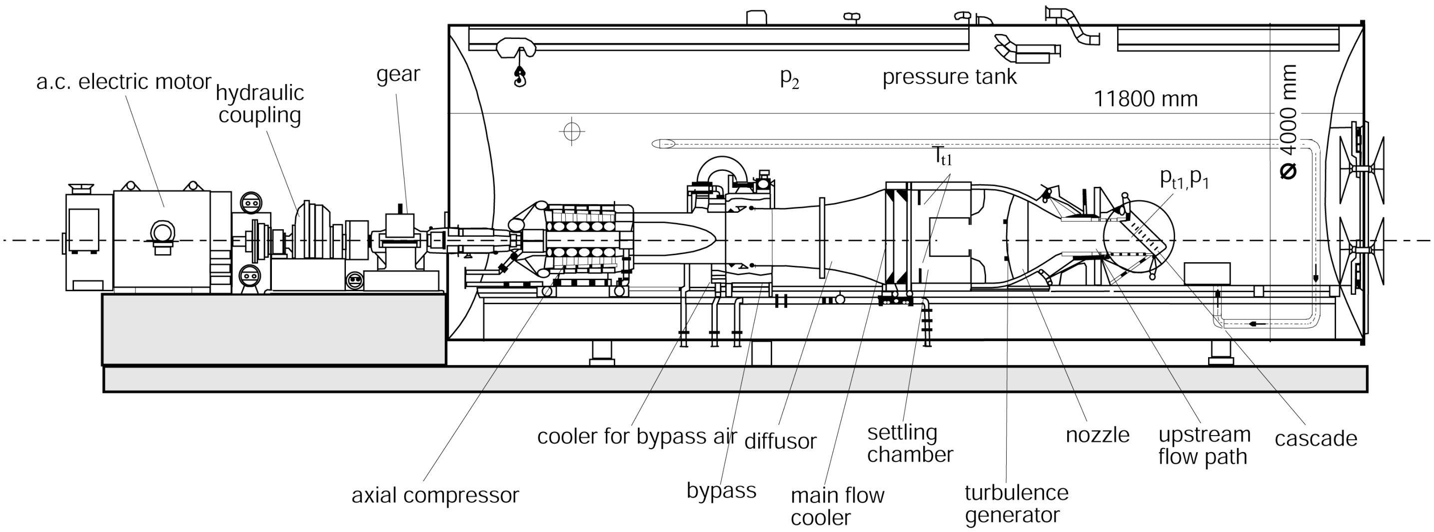

FIGURE 1. THE HIGH-SPEED CASCADE WIND TUNNEL

film cooling. Mick and Mayle [11] derived the heat flux ratio from eq. (3) and from the heat flux for the uncooled case

$$\dot{q}_0 = h_0 \cdot (T_w - T_\infty) \tag{5}$$

and obtain

$$\frac{\dot{q}}{\dot{q}_0} = \frac{h_c}{h_0} \cdot \left(1 - \frac{\eta}{\varphi}\right) \tag{6}$$

with

$$\varphi = \frac{T_w - T_\infty}{T_c - T_\infty}. \tag{7}$$

Since φ is a priori unknown a constant value of $\varphi = 0.6$ is assumed in many cases from open literature. What the authors forget to emphasize is that in both cases, with and without film cooling, the same wall and main flow temperature is assumed. In practice it will be difficult to achieve same temperatures on the wall in both cases without changing the coolant temperature and therefore φ. In fact if one looks closer to eq. (6) in the enumerator the heat flux definition for varying θ as in Choe et al. [9] is found, since φ is the reciprocal of θ as defined in eq. 4 and 7. This means that the heat flux ratio gives the needed heat flux with film cooling in order to obtain the same wall temperature as without film cooling for a given coolant temperature. But the heat flux into the blade changes also with changing wall temperature and a new equilibrium is established and therefore T_w can not remain constant when the heat flux is changed. In addition to that φ varies along the surface as was previously noted. In order to accurately predict the overall film cooling effectiveness a new parameter is derived in this paper. Using the heat transfer results presented in the first part of this paper [12] the overall effectiveness of film cooling on a highly loaded blade with flow separation is presented. The overall film cooling effectiveness is shown for variation of the operating point (exit Mach and Reynolds numbers) and of the coolant pressure ratio. Furthermore the influences of various parameters such as the geometry of the blade and convective heat transfer are shown.

MEASUREMENT SETUP

The experiments were conducted in the High-speed Cascade Wind Tunnel of the Institute of Jet Propulsion at the University of the German Federal Armed Forces Munich, shown in Fig. 1 and presented and explained in detail in Sturm and Fottner [13]. The wind tunnel operates continuously and major parts of it are enclosed inside a tank. The pressure inside the vessel can be varied in order to obtain an arbitrary Reynolds and Mach number combination. Vacuum pumps placed outside of the tank are used to create a constant static pressure inside of the tank between 3000 Pa and ambient pressure. A 1.3 MW electric motor, the hydraulic coupling and the gear, also located outside the tank, drive the six stage axial compressor inside the chamber. The flow pumped by the compressor passes through a cooler and the settling chamber before it is accelerated inside the nozzle towards the test section. At the entry of the nozzle a turbulence grid with crossed rectangular plates increases the turbulence level of the free stream to values of 4–5% at the entry into the cascade. The cascade placed at the end of the nozzle has an open end. The cascade outlet flow is blown into the environment of the pressure tank and reenters the axial compressor maintaining in such manner the same air recirculating inside the tank.

For experiments with film cooling the secondary air is sucked from the pressure tank by a screw compressor and introduced into the blades' plenum chambers. The coolant temperature is controlled before entering into the blades and can be changed between -30° C and the main flow temperature.

The main flow is kept at a constant temperature of $T_{t1} = 30^\circ$ C or 55° C for measurements of the heat transfer coefficient or of the adiabatic film cooling effectiveness respectively. The operating point (exit Mach and Reynolds numbers) is set controlling the ideal dynamic pressure $q_{2,s}$ — i.e. for adiabatic isentropic flow from inlet to outlet of the cascade — and the static

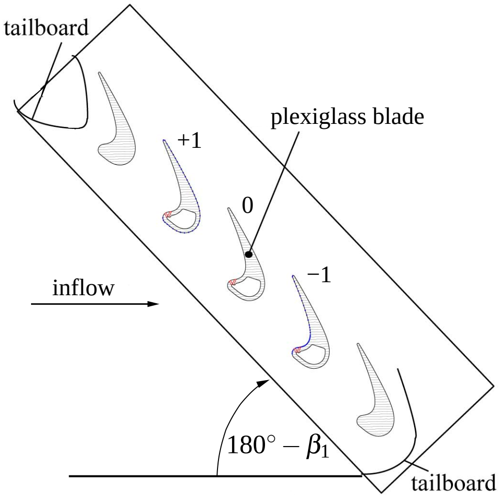

FIGURE 2. SCHEMATIC OF THE TEST SECTION AND CASCADE INSTRUMENTATION (NOT TO SCALE)

TABLE 1. GEOMETRIC AND AERODYNAMIC DATA OF THE T120C CASCADE

blade height to chord ratio	h/c	1.5
pitch to chord ratio	t/c	1.007
inlet Mach number	Ma_1	0.295
outlet Mach number	$\mathrm{Ma}_{2,s}$	0.87
outlet Reynolds number	$\mathrm{Re}_{2,s}$	$3.9 \cdot 10^5$
flow turning	$\Delta\beta$	120°
inlet angle	β_1	138.6°

pressure at the outlet p_2. The Mach number is defined by

$$\mathrm{Ma}_{2,s} = \sqrt{\frac{2}{\gamma-1} \cdot \left[\left(1 + \frac{q_{2,s}}{p_2}\right)^{\frac{\gamma-1}{\gamma}} - 1 \right]} \qquad (8)$$

and the Reynolds number, based on the true chord length c and using the Sutherland constants C_s and S to determine the dynamic viscosity, is defined by

$$\mathrm{Re}_{2,s} = \sqrt{\frac{\gamma}{R}} \frac{c}{C_s} \frac{\mathrm{Ma}_{2,s} \cdot p_2 \cdot \left(\frac{T_{t1}}{1+\left(\frac{\gamma-1}{2}\right)\cdot \mathrm{Ma}_{2,s}^2} + S \right)}{\left(\frac{T_{t1}}{1+\left(\frac{\gamma-1}{2}\right)\cdot \mathrm{Ma}_{2,s}^2} \right)^2}. \qquad (9)$$

Cascade Instrumentation

The T120C cascade consists of five blades in total, where the inner three are fed with air for film cooling, see Fig. 2. Adjustable tailboards are placed at the circumferential ends of the cascade, which gives five complete passages for the cascade and allows the creation of homogeneous inlet conditions. The main geometric parameters and aerodynamic data of the cascade at design conditions are given in Tab. 1, the definition of the geometry is shown in Fig. 3. The blade height to chord ratio is sufficient to have at mid passage no noticeable contraction of the stream tubes since the sidewall effects are relatively small. The film cooling design is shown in Fig. 4 and the data is listed in Tab. 2. In this cascade two rows of holes are placed on the pressure side with 21 holes in each row covering the whole span. The first row is located shortly after the stagnation line. The second row is placed inside the zone with main flow separation in order to reduce the extension of the separation bubble and to provide efficient film cooling to this zone. The three inner blades are film cooled in order to have periodic conditions for the inner passages and the plenum is sufficiently large to have similar coolant mass flow throughout the blade height.

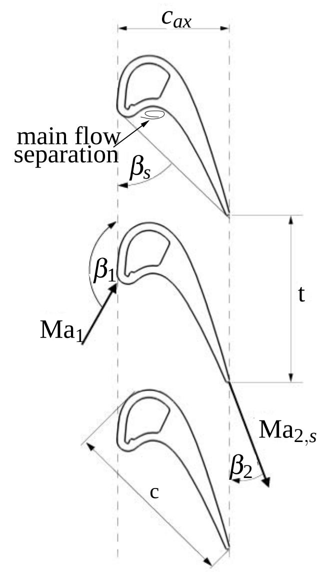

FIGURE 3. DEFINITION OF THE GEOMETRIC DATA ON THE T120C CASCADE (NOT TO SCALE)

TABLE 2. GEOMETRY OF THE FILM COOLING HOLES

		1st row	2nd row
relative axial position	x_{ax}/c_{ax}	0.118	0.198
relative hole pitch	$(t/D)_{fc}$	4	4
cylindrical part length	$(l_{cyl}/D)_{fc}$	3.4	1.9
fan-shaped part length	$(l_{fs}/D)_{fc}$	0	1.8
local angle to surface	α	82.7°	56.2°
compound angle	γ_r	37.1°	0°
fan-shape angle	γ_{fs}	0°	7.5°

The thermal measurements were carried out on the center blade (labeled as '0' in Fig. 2) which is made of plexiglass. At the two neighboring blades the profile pressure distribution is acquired with seventy static pressure taps. The suction side pressure is measured on the blade above the center blade (+1) and

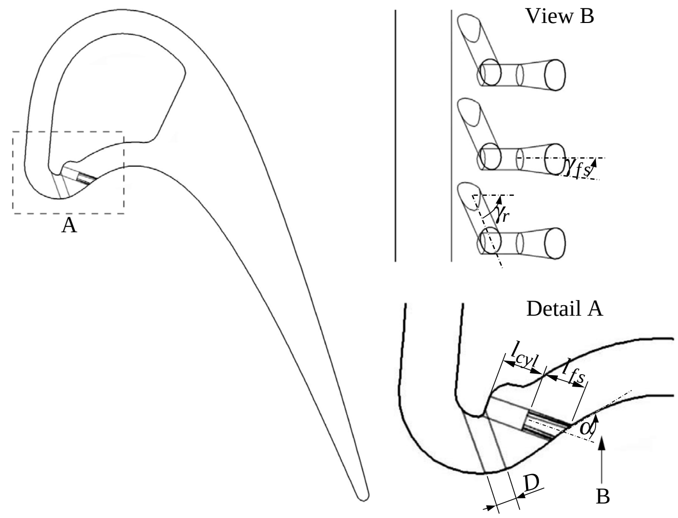

FIGURE 4. T120C BLADE AND DETAIL OF FILM COOLING (NOT TO SCALE)

the one on the pressure side on the blade below (-1). The static pressure $p(x)$ is plotted as isentropic Mach number on the blade

$$\mathrm{Ma}_s(x) = \sqrt{\frac{2}{\gamma-1} \cdot \left[\left(\frac{p_{t1}}{p(x)} \right)^{\frac{\gamma-1}{\gamma}} - 1 \right]}. \qquad (10)$$

For measurements of the heat transfer coefficient the pressure surface of the center blade is heated by a heating foil, the coolant temperature is kept equal to the main flow temperature $T_c = T_{t1}$ and the local heat transfer coefficient for isoenergetic condition is then obtained with

$$h(x,z) = \frac{\dot{q}}{T_w(x,z) - T_r(x)}. \qquad (11)$$

For the measurement of the adiabatic film cooling effectiveness the coolant temperature is cooled and the effectiveness is defined by

$$\eta(x,z) = \frac{T_r(x) - T_{aw}(x,z)}{T_{t1} - T_c}. \qquad (12)$$

A finite element analysis is carried out in order to account for the heat conduction inside the blade. Since high velocities are present the recovery temperature has to be used for determination of h and η. The recovery temperature $T_r(x)$ is calculated using the adiabatic-isentropic velocity $u(x)$ from profile pressure measurements with

$$T_r(x) = T_{t1} + (r-1) \cdot \frac{u(x)^2}{2 \cdot c_p} \qquad (13)$$

with the recovery factor defined by $r = \mathrm{Pr}^{1/2}$ for laminar and $r = \mathrm{Pr}^{1/3}$ for turbulent flow. The total inlet temperature T_{t1} is

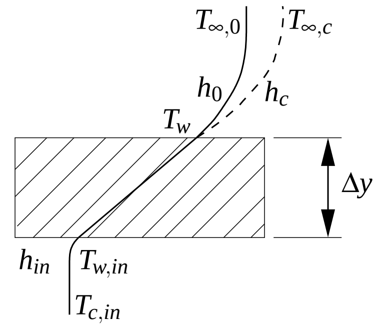

FIGURE 5. ONE-DIMENSIONAL HEAT FLUX IN THE BLADE

measured inside the settling chamber with four PT100 class A resistance thermometers. For measurements with film cooling the coolant total temperature T_c is measured with a PT100 inside the plenum. Details on the measurement technique can be found in previous publications [4, 5, 12].

Measurement Uncertainty The uncertainty for the main flow temperature was estimated to be of ± 0.3 K and ± 0.4 K was used for the plenum temperature. For the surface temperature a calibration error of ± 0.3 K plus the uncertainty due to the image acquisition is taken into account. Latter is influenced among others by the intensity of the camera signals. This results in overall to an uncertainty of 10–20% of the measured heat transfer coefficient and of 5–20% for the adiabatic film coling effectiveness. Since the repeatability of the measurements is much higher, comparisons between different measurements can be done with a maximum uncertainty of about 5%, combining the unceratinaty of the measurements of the heat transfer and adiabatic film cooling effectiveness.

For the isentropic Mach number $Ma_s(x)$ the uncertainty is estimated to be lower than 0.5%.

EVALUATION OF AN OVERALL FILM COOLING EFFECTIVENESS

As was explained in the introduction, the widely used heat flux ratio or alternatively the net heat flux reduction seem not to be an ideal parameter in order to evaluate the effect of film cooling on a non-adiabatic blade. In Gomes [14] a new parameter is derived which is called temperature difference ratio (TDR) and is here briefly explained with the aid of fig. 5. The assumptions used for the TDR are following:

The local wall temperature $T_w(x,z)$ is equal with and without film cooling, e. g. the maximum temperature allowed for the blade.

The main flow temperature can change. The goal behind the film cooling would then be to increase the inlet temperature by keeping the wall temperature constant.

The heat flux into the blade is one-dimensional and constant since the parameters driving the heat flux are not changed, i. e. outer wall temperature T_w, inner wall temperature $T_{w,in}$, blade geometry and internal heat transfer coefficient for convective cooling h_{in}.

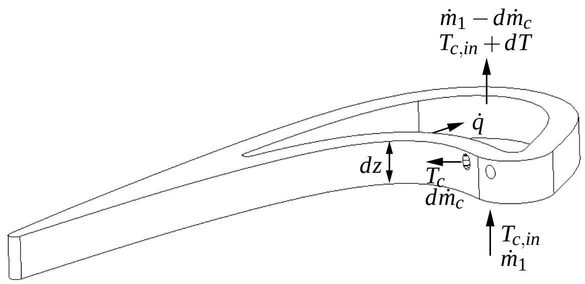

FIGURE 6. BLADE WITH FINITE EXTENSION IN SPANWISE DIRECTION

The material of the blade has constant and isotropic properties and no thermal barrier coating is applied to the surface.

With these assumptions the following relations are obtained:

$$\begin{aligned}\dot{q} &= h_0 \cdot (T_w - T_{\infty,0}) \\ &= \frac{k}{\Delta y} \cdot (T_{w,in} - T_w) \\ &= h_{in} \cdot (T_{c,in} - T_{w,in}) \\ &= h_c \cdot (T_w - T_{aw})\end{aligned} \tag{14}$$

with the heat conductivity k and the thickness Δy of the blade for a slice of the blade dz as is shown in fig 6. Setting T_{aw} from eq. (1) in eq. (14),but with $T_{\infty,c}$ instead of T_∞ in order to be able to distinguish between the main flow temperatures with and without film cooling, following equation is obtained:

$$h_0 \cdot (T_w - T_{\infty,0}) = h_c \cdot [T_w - T_{\infty,c} + \eta\,(T_{\infty,c} - T_c)]\,. \tag{15}$$

$T_{c,in}$ is the coolant temperature inside the cavity. The coolant is heated before it exits the film cooling hole with the temperature T_c and the relation between the temperatures will in most cases be $T_w > T_{w,in} > T_c > T_{c,in}$. These four temperatures change along the blade span, but for a cut of the blade with finite thickness dz these temperatures can be regarded as constant. For the further evaluation $T_{w,in}$ is needed and it can be substituted by $T_{w,in} = \xi \cdot T_c$. The coolant temperature T_c can then be obtained also from eq. (14) as

$$T_c = \frac{\frac{h_0}{K_1}\,(T_w - T_{\infty,0}) + T_w}{\xi} \tag{16}$$

with the constant $K_1 = k/\Delta y$. Introducing the temperature difference ratio TDR defined by

$$TDR = \frac{T_w - T_{\infty,0}}{T_w - T_{\infty,c}} \tag{17}$$

and combining eq. (16) with eq. (15) following relation is obtained

$$TDR = \frac{h_c}{h_0}\frac{1 - \eta\left(1 - \frac{(1-1/\xi)}{1 - T_{\infty,c}/T_w}\right)}{1 + \frac{h_c}{K_1}\frac{\eta}{\xi}}. \tag{18}$$

TABLE 3. MEASUREMENT MATRIX BASED ON OUTLET CONDITIONS

case	$Ma_{2,s}$	$Re_{2,s}$	$p_{t,c}/p_{t,1}$
1	0.87	390,000	0, 1.03, 1.09, 1,12
2	0.87	800,000	0, 1.03, 1.09
3	0.95	390,000	0, 1.03, 1.09

The film cooling has then a positive effect wherever TDR is smaller than unity. In Gomes [14] a more detailed explanation of the derivation is given for $\xi = 1$. For compressible flow the recovery temperature T_r is used instead of T_∞ in eq. 5 and after some derivation the following equation is obtained:

$$TDR = \frac{h_c}{h_0}\frac{1 - \eta\left(1 - \frac{(1-1/\xi)}{1 - T_{r,c}/T_w} - \frac{\frac{u^2}{2c_p}(1-r)}{T_w - T_{r,c}}\right)}{1 + \frac{h_c}{K_1}\frac{\eta}{\xi}}. \tag{19}$$

In most relevant cases eq. 19 can be simplified to

$$TDR \approx \frac{h_c}{h_0}\frac{1 - \eta\left(1 - \frac{(1-1/\xi)}{1 - T_{r,c}/T_w}\right)}{1 + \frac{h_c}{K_1}\frac{\eta}{\xi}} \tag{20}$$

as it will be shown in the following.

RESULTS

The heat transfer and adiabatic film cooling effectiveness were measured on the pressure side of the T120C blade for three different outlet conditions as indicated in tab. 3. The heat transfer coefficient was measured for the three operating points without film cooling. In that case a blade with holes is used and the plenum is sealed against the ambient. Since the pressure difference between the holes is very small almost no cross flow between them is present. Furthermore up to three blowing ratios were run for experiments with film cooling. The parameter used here is the ratio between total coolant and total inlet pressure $p_{t,c}/p_{t,1}$. Ratios of 1.03 and 1.09 and additionally of 1.12 for the design point (case 1) were run. With those pressure ratios blowing ratios between 2 and 4 are obtained. The isentropic Mach number on the blade is shown in fig. 7 for the three operating points. The computed values for the design case is shown as solid line. The flow on the suction side is transonic with weak shocks. On the pressure side, flow separation is visible from $x_{ax}/c_{ax} \approx 0.15$ up to 0.45. After reattachment the flow is strongly accelerated with an acceleration parameter $K = \frac{\nu}{u^2} \cdot \frac{du}{dx}$ constantly over the critical value for relaminarization of $3 \cdot 10^{-6}$, see Mayle [15]. The RANS computation agrees very well with the measurements. Especially on the suction side the transition is predicted correctly. On the pressure side the separation zone is larger in the simulation than the measured one. Near-wall flow visualizations with oil-and-dye technique confirmed the separation and reattachment lines at 0.15 and 0.45 respectively, refer to Gomes [14].

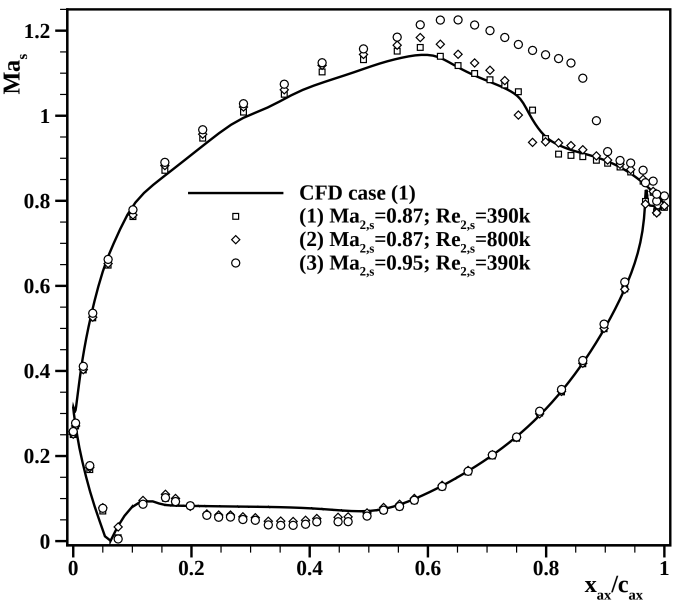

FIGURE 7. ISENTROPIC MACH NUMBER ON THE BLADE

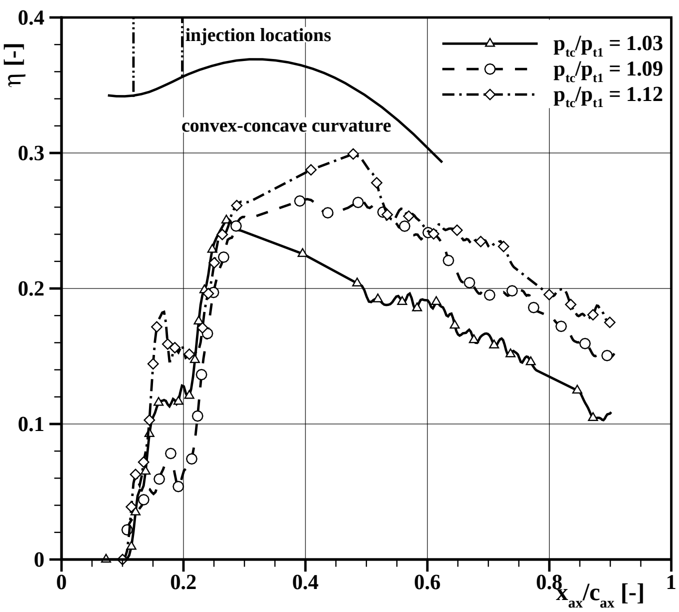

FIGURE 8. ADIABATIC FILM COOLING EFFECTIVENESS FOR $\mathrm{Ma}_{2,s} = 0.87$, $\mathrm{Re}_{2,s} = 390,000$

Evaluation of the Overall Film Cooling Effectiveness

In order to be able to analyze in more detail the overall film cooling effectiveness, some results from Gomes and Niehuis [4] are repeated in fig. 8 with the adiabatic film cooling effectiveness plotted as function of the axial chord for the design operating point at three different coolant pressure ratios. One can see indications of jet detachment close to the ejection locations and high film cooling effectiveness at about mid chord, a region where the jets impinge on the surface. Further downstream the coolant is mixed out with the main flow.

In order to obtain the coolant effect on a non-adiabatic blade the temperature difference ratio is built for the different operating points and coolant pressure ratios. The TDR is a function of

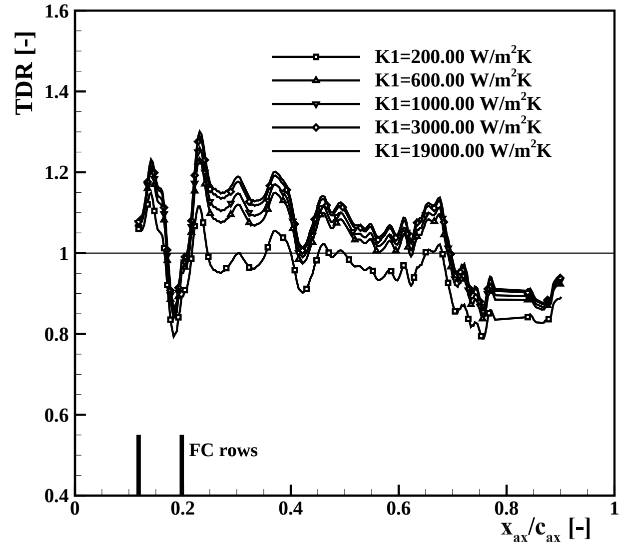

FIGURE 9. TDR FOR $\mathrm{Ma}_{2,s} = 0.87$, $\mathrm{Re}_{2,s} = 390,000$, $p_{tc}/p_{t1} = 1.03$, $r = 1$ and $\xi = 1$; VARIATION OF K_1

measured values h_c, h_0 and η as well as of variables depending on the geometry and material of the blade K_1, on the heat transfer on the inner side of the blade ξ and $T_{r,c}/T_w$, refer to eq. (18). Therefore an evaluation of the influence of these variables on the TDR for the measurements is carried out. First let us consider a simpler case with $\xi = 1$ and $r = 1$. In that case eq. (19) reduces to

$$TDR = \frac{h_c}{h_0} \frac{1-\eta}{1+\frac{h_c \cdot \eta}{K_1}}. \tag{21}$$

The influence of K_1 on the TDR is shown in fig. 9 for the design operating point and $p_{tc}/p_{t1} = 1.03$ by simply computing eq.(21) using the measured values for η, h_c and h_0 and changing the values of K_1. It is visible that the parameter K_1 has a negligible influence on the TDR if $K_1 > 3000\,\mathrm{W}/\left(\mathrm{m}^2 \cdot \mathrm{K}\right)$. For a conductivity of $k = 25\,\mathrm{W}/(\mathrm{m} \cdot \mathrm{K})$, which is a realistic value for nickel based alloys (see [16]) this is true for a thickness of the blade of $\Delta y < 8.3\,\mathrm{mm}$, which should be the case for most of the used airfoils in jet engines. Analyzing in more detail fig. 9 the effect of varying K_1 is quite logical: the less conductive the material is the less heat flux is present and the film cooling gains more importance. This effect should be taken into account when using thermal barrier coating with decreased thermal conductivity. The heat flux ratio does not differentiate between different heat fluxes into the blade and might lead to wrong conclusions.

Let us now consider a more realistic case with varying ξ in fig. 10. Therefore the TDR was computed for the reference operating point at $p_{tc}/p_{t1} = 1.03$. The wall temperature T_w and the coolant temperature T_c were set to values of 1250 and 850 K respectively with $K_1 = 8000\,\mathrm{W}/\left(\mathrm{m}^2 \cdot \mathrm{K}\right)$ and $r = 1$. The temperature values seem to be realistic for a turbine. For varying ξ the temperature ratio $T_{r,c}/T_w$ is then computed in order to fulfill eq. (14). The curves are labeled with the appropriate factor ξ and the resultant heat transfer coefficient on the inside of the wall h_{in} computed for $T_{c,in} = T_c$. For the plot the curves were selected based on more or less realistic values of the resultant h_{in}. The

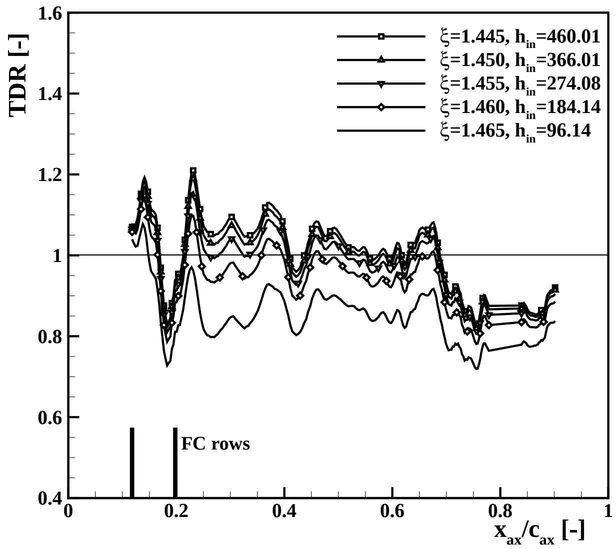

FIGURE 10. TDR FOR $\mathrm{Ma}_{2,s} = 0.87$, $\mathrm{Re}_{2,s} = 390{,}000$, $p_{tc}/p_{t1} = 1.03$, $r = 1$ and $K1 = 8000$; VARIATION OF ξ

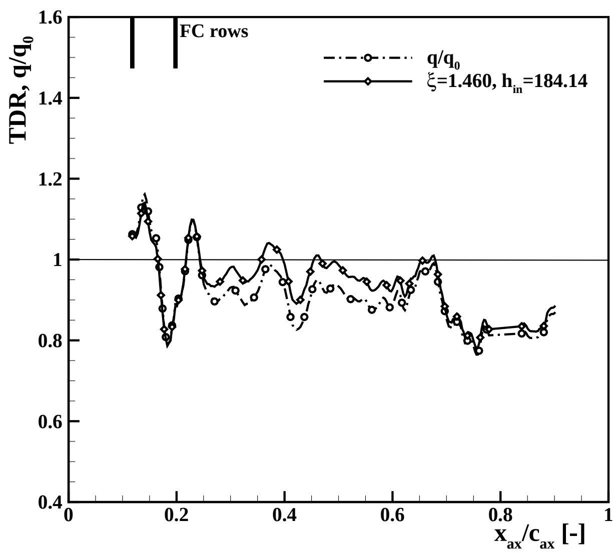

FIGURE 11. TDR FOR $\mathrm{Ma}_{2,s} = 0.87$, $\mathrm{Re}_{2,s} = 390{,}000$, $p_{tc}/p_{t1} = 1.03$, $r = 1$ and $K1 = 8000$ COMPARED TO HEAT FLUX RATIO

increase of $T_{w,in}$ leads to a reduction of the heat flux and has a similar effect as the reduction of K_1 in the previous plot with an increase of the positive effect of the film cooling. Also here the additional variation of K_1 down to $3000\,\mathrm{W}/\left(\mathrm{m}^2\cdot\mathrm{K}\right)$ has no significant effect on TDR. For average internal heat transfer coefficients $h_{in} > 270\,\mathrm{W}/\left(\mathrm{m}^2\cdot\mathrm{K}\right)$ the influence of varying h_{in} is relatively small. This influence is even more reduced with decreasing values of K_1.

Finally the influence of compressibility on TDR can be assessed by a simple calculation. For $T_{t1} = 1950\,\mathrm{K}$, $T_w = 1250\,\mathrm{K}$, sonic velocity and $r = 0.87$ one obtains $\frac{u^2}{2c_p}(1-r)/(T_w - T_{r,c}) = 0.087$ and therefore a difference between eq. (19) and the simpler eq. (20) of less than $8.7\ \% \cdot \eta$. For the cases under consideration on the pressure side of the T120C blade, the differences are smaller than the line thickness and are therefore not shown in a plot.

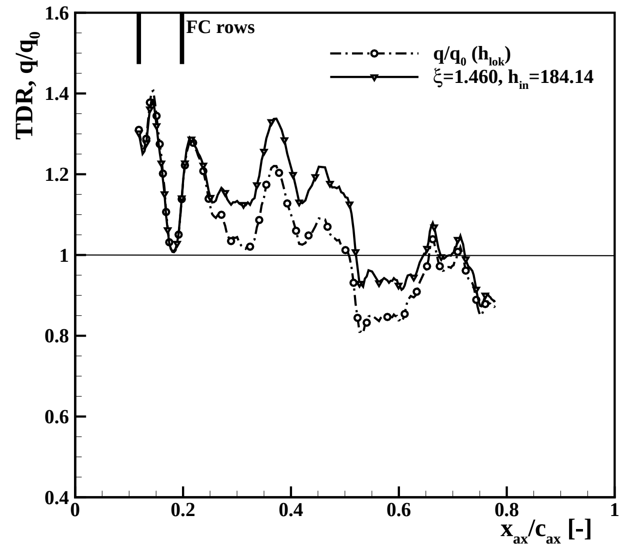

FIGURE 12. TDR FOR $\mathrm{Ma}_{2,s} = 0.95$, $\mathrm{Re}_{2,s} = 390{,}000$, $p_{tc}/p_{t1} = 1.09$, $r = 1$ and $K1 = 8000$ COMPARED TO HEAT FLUX RATIO

The comparison between the temperature difference ratio and the heat flux ratio q/q_0 is given in fig. 11 in order to evaluate the difference between both parameters. The curve for $\xi = 1.46$ was chosen because it offers the best fit to the curve for the heat flux ratio and gives quite realistic internal HTC and temperature values. As can be seen the curves deviate especially in the middle region between $0.25 < x_{ax}/c_{ax} < 0.6$. Reason for this difference between TDR and the heat flux ratio is that in this region φ computed from $T_{r,c}/T_w$ is larger than 0.6 and therefore the constant value assumed for φ in order to build the heat flux ratio. The reason why in the other regions the differences are small is because upstream of $x_{ax}/c_{ax} = 0.25$ the film effectiveness is too small in order to have a visible effect and for $x_{ax}/c_{ax} > 0.6$ the ratio h_c/h_0 is almost unity.

Larger differences between the TDR and the heat flux ratio are seen for the high Mach number case at $p_{tc}/p_{t1} = 1.09$ in Fig. 12. Here differences of up to 20% are seen since the difference in the heat transfer with and without film cooling inside the separation bubble is much larger than for the design operating point. While using the heat flux ratio one might tend to use film cooling the decision based on the TDR would be clearly negative. Nevertheless one should be aware that the comparisons of Fig. 11 and Fig. 12 are only the best fit between both curves. Setting the true values of the blade K_1 and ξ might give stronger differences between both methods. A precise calculation would also consider varying blade wall thickness Δy and internal heat transfer coefficient h_{in} along the chord. In these investigations, however, the goal is not to give a precise evaluation for defined conditions but to give a general overview on the influences of the different factors.

Influence of Operating Point and Blowing Ratio on the Temperature Difference Ratio Having analyzed the influence of geometric and internal cooling parameters on TDR the influences of different operating points and blowing ratios are analyzed here. The chosen values for ξ and K_1 remain 1.46 and $8000\,\mathrm{W}/\left(\mathrm{m}^2\cdot\mathrm{K}\right)$, since quite realistic values were obtained for

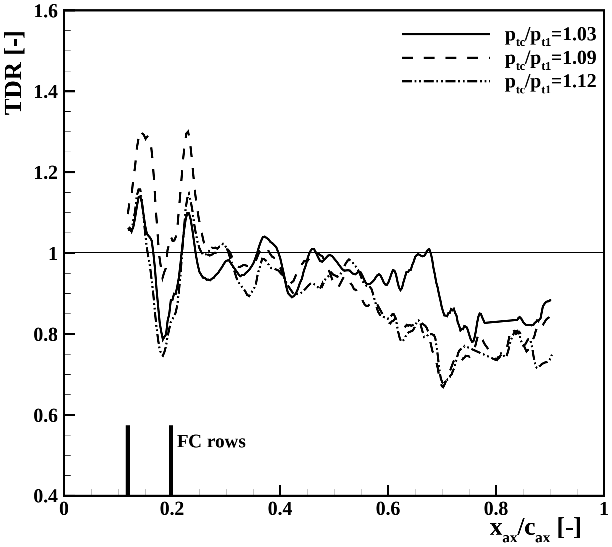

FIGURE 13. TDR FOR $\mathrm{Ma}_{2,s} = 0.87$, $\mathrm{Re}_{2,s} = 390,000$

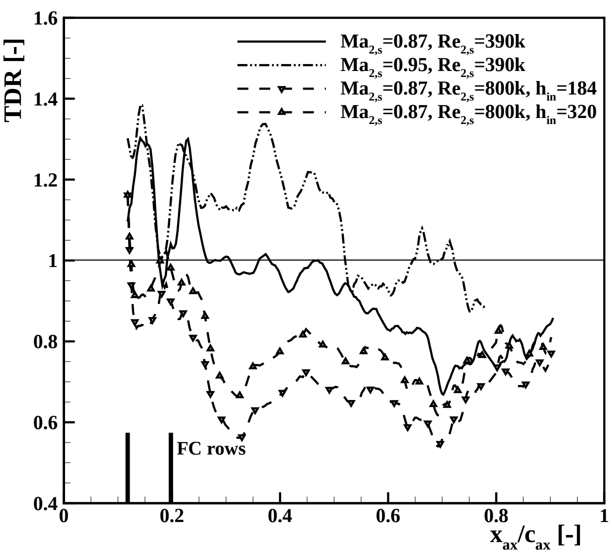

FIGURE 14. TDR FOR $p_{tc}/p_{t1} = 1.09$

$T_{w,in}$ and h_{in} with the chosen boundary conditions. The recovery factor is set to $r = 1$. The TDR for the design operating point at different coolant pressure ratios is shown in fig. 13. The jet detachment at the ejection location and consequently low adiabatic film cooling effectiveness at the middle pressure ratio is reflected in high values of TDR. Toward the trailing edge the enhanced film cooling at higher blowing ratios leads to TDR values below 1 and therefore positive effect of film cooling. Within the flow separation region it is difficult to achieve a positive effect of the film cooling due to the increased heat transfer. The optimum pressure ratio at this exit Mach and Reynolds numbers seems to be at $p_{tc}/p_{t1} = 1.12$ but no remarkable changes inside the separation zone are achieved and potentials for optimization of the film cooling in this region are identified.

The TDR for different operating points at $p_{tc}/p_{t1} = 1.09$ is plotted in fig. 14. The larger heat transfer increase inside the separation zone at the higher exit Mach number is reflected in high values of TDR in this region while for the high Reynolds number the heat transfer augmentation is more reduced and the adiabatic film cooling effectiveness increased. This results in a more positive effect of film cooling at the higher Reynolds number. For the high exit Reynolds number two curves are shown, one with the same ξ as for the other two and a second one with the internal heat transfer coefficient h_{in} scaled by $\mathrm{Re}_{2,s}^{0.8}$ which should allow the more realistic comparison since the internal heat transfer also increases with fluid density. With higher heat flux at $\mathrm{Re}_{2,s} = 800,000$ the positive effect of film cooling is reduced but is still perceived along the whole measured extension.

It can therefore be concluded that film cooling is beneficial at higher Reynolds number where a smaller flow separation and higher heat transfer without film cooling occurs. At lower Reynolds number with larger flow separation the heat transfer augmentation with film cooling is very high and the adiabatic film cooling effectiveness is too low leading to a stronger heating of the blade.

SUMMARY

A new parameter called temperature difference ratio TDR is introduced, which allows to evaluate the film cooling effectiveness on a non-adiabataic wall. This parameter is suitable for using with measurements of the adiabatic film cooling effectiveness and of the heat transfer coefficient at isoenergetic conditions. It is valid for compressible flow with defined wall geometry, wall material and heat transfer on the opposite wall to the film cooled surface and a given linearity of the energy equation with temperature. It corrects some deficits of the often used heat flux ratio or net heat flux reduction, such as assuming a constant non-dimensionalized wall temperature $\varphi = (T_w - T_\infty)/(T_c - T_\infty)$, and it is able to assess the real occurrences on a blade such as a reduction of the heat flux with reduced wall temperature due to film cooling.

It is shown that the film cooling effectiveness is strongly related to the heat flux into the blade which itself is dependent on the heat transfer in the interior of the blade, the blade geometry and heat conductivity, though the influence is reduced at higher values of conductivity and smaller wall thickness. An assessment of the film cooling effect might therefore have to take into account such parameters. The method described in this paper using the temperature difference ratio also allows to be used for a more detailed design and optimization of airfoils without extensive numerical calculations simply by coupling correlations from measurements with different internal blade designs.

In the results shown here, film cooling inside the separation bubble turns out to be difficult since the heat transfer is strongly enhanced by the turbulent mixing of the jets with the main flow. Only at the high Reynolds number is a positive effect of film cooling along the whole chord of the blade achieved. At lower Reynolds number the film cooling leads to a negative effect close to the ejection holes and, for the high Mach number, also inside the separation zone. Future blade designs might therefore focus more on the reduction of the external heat transfer coefficient when the heat conductivity inside the blade is high.

Using thermal barrier coating and having therefore low heat conductivity inside the blade, it was shown that the film cooling has more positive effects and the focus of the cooling design would then change.

ACKNOWLEDGMENT

The results presented here were carried out within the EU-founded AITEB-2 project no. AST4-CT-2005-516113. The permission to publish is acknowledged by the authors and they express herewith their gratitude to the partners for the collaboration.

REFERENCES

[1] Han, J.-C., Dutta, S., and Ekkad, S. V., 2000. *Gas Turbine Heat Transfer and Cooling Technology*. Taylor and Francis, New York. ISBN: 1-56032-841-X.

[2] Haselbach, F., and Schiffer, H., 2004. "Aerothermal investigations on turbine endwalls and blades". In Proceedings of the ASME Turbo Expo 2004, no. GT2004-53078.

[3] Janke, E., and Wolf, T., 2010. "Aerothermal research for turbine components — an overview of the european AITEB-2 project". In Proceedings of the ASME Turbo Expo 2010, no. GT2010-23511.

[4] Gomes, R., and Niehuis, R., 2009. "Film cooling effectiveness measurements on highly loaded blades with flow separation". In Proceedings of the 8th European Conference on Turbomachinery, Fluid Dynamics and Thermodynamics (ETC), no. 237.

[5] Gomes, R. A., and Niehuis, R., 2011. "Film Cooling Effectiveness Measurements With Periodic Unsteady Inflow on Highly Loaded Blades With Main Flow Separation". *Journal of Turbomachinery*, ***133***, April, pp. 021019–1–021019–11.

[6] Camci, C., and Arts, T., 1990. "An Experimental Convective Heat Transfer Investigation Around a Film-Cooled Gas Turbine Blade". *Journal of Turbomachinery*, ***112***, pp. 497–503.

[7] Abhari, R. S., and Epstein, A., 1992. "An Experimental Study of Film Cooling in a Rotating Transonic Turbine". In Proceedings of the International Gas Turbine and Aeroengine Congress and Exposition, no. 92-GT-201, ASME.

[8] Eckert, E., 1984. "Analysis of Film Cooling and Full-Coverage Film Cooling of Gas Turbine Blades". *Journal of Engineering for Gas Turbines and Power*, ***106***, pp. 206–213.

[9] Choe, H., Kays, W., and Moffat, R., 1974. "The Superposition Approach to Film-Cooling". In Proceedings of the Winter Annual Meeting, no. 74-WA/HT-27, ASME.

[10] Metzger, D., Carper, H., and Swank, L., 1968. "Heat Transfer With Film Cooling Near Nontangential Injection Slots". *Journal of Engineering for Power*, ***90***, pp. 157–163.

[11] Mick, W., and Mayle, R., 1988. "Stagnation Film Cooling and Heat Transfer, Including Its Effect Within the Hole Pattern". *Journal of Turbomachinery*, ***110***, pp. 66–72.

[12] Gomes, R. A., and Niehuis, R., 2011. "Film cooling on highly loaded blades with main flow separation - part 1: Heat transfer". In Proceedings of the ASME Turbo Expo 2011, no. GT2011-45476.

[13] Sturm, W., and Fottner, L., 1985. "The High-Speed Cascade Wind-Tunnel of the German Armed Forces University Munich". In 8th Sympsium on Measuring Techniques for Transonic and Supersonic Flows in Cascades and Turbomachines.

[14] Gomes, R. A., 2010. "On Aerothermal Effects of Film Cooling on Turbine Blades with Flow Separation". PhD thesis, Universität der Bundeswehr München. ISBN:978-3-86853-600-3.

[15] Mayle, R. E., 1991. "The Role of Laminar-Turbulent Transition in Gas Turbine Engines". *Journal of Turbomachinery*, ***113***, pp. 509–537.

[16] Verein Deutscher Ingenieure, ed., 2002. *VDI-Wärmeatlas*, ninth ed. Springer Verlag, Berlin. ISBN: 3-540-41200-X.